Electronic damage in S atoms in a native protein crystal induced by an intense X-ray free-electron laser pulse

L. Galli, S.-K. Son, M. Klinge, S. Bajt, A. Barty, R. Bean, C. Betzel, K. R. Beyerlein, C. Caleman, R. B. Doak, M. Duszenko, H. Fleckenstein, C. Gati, B. Hunt, R. A. Kirian, M. Liang, M. H. Nanao, K. Nass, D. Oberthür, L. Redecke, R. Shoeman, F. Stellato, C. H. Yoon, T. A. White, O. Yefanov, J. Spence, and H. N. Chapman

Citation: Structural Dynamics **2**, 041703 (2015); doi: 10.1063/1.4919398
View online: http://dx.doi.org/10.1063/1.4919398
View Table of Contents: http://scitation.aip.org/content/aca/journal/sdy/2/4?ver=pdfcov
Published by the American Crystallographic Association, Inc.

STRUCTURAL DYNAMICS **2**, 041703 (2015)

Electronic damage in S atoms in a native protein crystal induced by an intense X-ray free-electron laser pulse

L. Galli,[1,2] S.-K. Son,[1,3] M. Klinge,[4] S. Bajt,[5] A. Barty,[1] R. Bean,[1] C. Betzel,[6] K. R. Beyerlein,[1] C. Caleman,[1,7] R. B. Doak,[8] M. Duszenko,[9] H. Fleckenstein,[1] C. Gati,[1] B. Hunt,[10] R. A. Kirian,[1,a)] M. Liang,[1,b)] M. H. Nanao,[11] K. Nass,[8] D. Oberthür,[1] L. Redecke,[4] R. Shoeman,[8] F. Stellato,[1,c)] C. H. Yoon,[1,12] T. A. White,[1] O. Yefanov,[1] J. Spence,[13] and H. N. Chapman[1,2,3,d)]

[1]*Center for Free-Electron Laser Science, Deutsches Elektronen-Synchrotron DESY, Notkestrasse 85, 22607 Hamburg, Germany*
[2]*Department of Physics, University of Hamburg, Jungiusstr. 6, 20355 Hamburg, Germany*
[3]*The Hamburg Centre for Ultrafast Imaging, Luruper Chaussee 149, 22761 Hamburg, Germany*
[4]*Joint Laboratory for Structural Biology of Infection and Inflammation, Institute of Biochemistry and Molecular Biology, University of Hamburg and Institute of Biochemistry, University of Luebeck at DESY, 22607 Hamburg, Germany*
[5]*Photon Science, Deutsches Elektronen-Synchrotron DESY, Notkestrasse 85, 22607 Hamburg, Germany*
[6]*Department of Chemistry, Institute of Biochemistry and Molecular Biology, University of Hamburg at DESY, 22607 Hamburg, Germany*
[7]*Department of Physics and Astronomy, Uppsala University, Box 516, 75120 Uppsala, Sweden*
[8]*Department of Biomolecular Mechanisms, Max Planck-Institute for Medical Research, Jahnstrasse 29, 69120 Heidelberg, Germany*
[9]*Interfaculty Institute of Biochemistry, University of Tübingen, 72076 Tübingen, Germany*
[10]*Department of Physics and Astronomy, Brigham Young University, Provo, Utah 84602, USA*
[11]*EMBL, Grenoble Outstation, Rue Jules Horowitz 6, Grenoble 38042, France*
[12]*European XFEL GmbH, Albert Einstein Ring 19, 22761 Hamburg, Germany*
[13]*Department of Physics, Arizona State University, Tempe, Arizona 85287-1504, USA*

(Received 12 March 2015; accepted 17 April 2015; published online 29 April 2015)

Current hard X-ray free-electron laser (XFEL) sources can deliver doses to biological macromolecules well exceeding 1 GGy, in timescales of a few tens of femtoseconds. During the pulse, photoionization can reach the point of saturation in which certain atomic species in the sample lose most of their electrons. This electronic radiation damage causes the atomic scattering factors to change, affecting, in particular, the heavy atoms, due to their higher photoabsorption cross sections. Here, it is shown that experimental serial femtosecond crystallography data collected with an extremely bright XFEL source exhibit a reduction of the effective scattering power of the sulfur atoms in a native protein. Quantitative methods are developed to retrieve information on the effective ionization of the damaged atomic species from experimental data, and the implications of utilizing new phasing methods which can take advantage of this localized radiation damage are discussed. [http://dx.doi.org/10.1063/1.4919398]

[a)]Present address: Department of Physics, Arizona State University, Tempe, Arizona 85287-1504, USA.
[b)]Present address: SLAC National Accelerator Laboratory, 2575 Sand Hill Road, Menlo Park, California 94025, USA.
[c)]Present address: I.N.F.N. Sezione di Rome "Tor Vergata," Roma 00133, Italy.
[d)]Author to whom correspondence should be addressed. Electronic mail: henry.chapman@cfel.de

I. INTRODUCTION

The sulfur single-wavelength anomalous diffraction (S-SAD) phasing method allows the determination of native protein structures without requiring chemical modification or the knowledge of a homologous structure. However, this *de novo* phasing technique presents its own problems arising from the long 5.02 Å wavelength at which the sulfur K-edge lies at 2.47 keV photon energy. To resolve structural features at near-atomic resolution (2 Å or higher) using diffraction at scattering angles less than 90°, a diffraction experiment must be carried out at a photon energy higher than about 6 keV. At this wavelength, the Bijvoet differences upon which the S-SAD phasing relies are very weak: for a typical protein containing a single sulfur atom for every 30 residues, the average difference is about 2% at 6 keV. Low anomalous signal requires the collection of very accurate data, which often means longer acquisition times (exacerbated by strong air absorption) and consequently a higher risk of radiation damage effects. The difficulty of the technique is also demonstrated by the very low number of deposited structures solved with S-SAD, compared to other X-ray methods (124 vs. 94 474: Results from queries dated 09/02/15 using the Protein Data Bank website (www.pdb.org). For S-SAD, the advanced search "Structure Determination Method" was used, in combination with "Text search." Due to the absence of well-defined S-SAD search criteria, this number could be an underestimate). Son *et al.* (2011a; 2011b) postulated that at high-intensity, X-ray free-electron laser (XFEL) radiation can ionize a significant population of the atoms of the sample during the X-ray pulse, and that heavy atoms are more strongly affected due to their higher photoabsorption cross sections. Furthermore, it was predicted that standard anomalous phasing methods would be frustrated under these conditions, because the absorption edges of the ions created during the XFEL pulse shift towards higher energies. These effects have been observed in recent experiments (Nass *et al.*, 2015 and Galli *et al.* unpublished). In particular, Nass *et al.* (2015) observed indications of electronic damage localized on the iron-sulfur clusters of ferredoxin protein crystals. Similarly, Galli *et al.* (unpublished) showed a moderate reduction of the scattering strengths of Gd atoms contained in a derivative protein crystal at high X-ray fluence, as well as a degradation of the quality of the experimental phasing that could be obtained. In the case of SAD, indeed, the theory presented in the paper of Son *et al.* predicts a reduction of the out-of-phase component of the atomic form factor proportional to the incident X-ray intensity, which would complicate anomalous phasing methods (Barends *et al.*, 2014). However, this theory also predicts a large amount of ionization of the heavy atoms at high intensities, which would increase the difference in the scattering strengths of these atoms for different fluences. By acquiring data at more than a single X-ray fluence, one could therefore exploit the change of scattering factors of the heavy atoms to retrieve their positions. Son *et al.* (2011a; 2011b) also derived new equations that could be used, similar to the case of MAD (multi-wavelength anomalous dispersion), to solve the phase problem *ab initio*. This new phasing technique is not limited by the chosen wavelength. Longer wavelengths will generally enhance the effect of ionization, whereas shorter wavelengths may allow higher-resolution diffraction. The main requirement is that the pulse fluence be sufficient to induce moderate ionization effects. In a previous paper (Galli *et al.*, 2015), simulations of serial femtosecond crystallography (SFX) experiments showed that the available XFEL sources such as the Linac Coherent Light Source (LCLS) should provide enough photon flux to saturate sulfur ionisation at a photon energy of 6 keV, and that by reducing the highest accessible flux by about two orders of magnitude it should be possible to utilize a high fluence (HF) version of the conventional radiation-induced phasing (RIP) (Ravelli *et al.*, 2003) workflow to obtain good quality phases of a native protein system. Here, a high intensity XFEL experiment on the actual native protein that was used for the reported simulations is described, allowing for a comparison between theory and experiment.

II. EXPERIMENT

A. Sample

The native protein sample employed for this experiment was Cathepsin B (CatB) — an enzyme belonging to the class of cysteine proteases which degrade polypeptides. The form of

the enzyme used is specific to the *Trypanosoma brucei* (Tb) parasite. The structure of the glycosylated form of TbCatB was recently solved using the SFX method (Redecke *et al.*, 2013). TbCatB crystals used in this study were grown inside living *Spodoptera frugiperda* insect cells infected by a recombinant baculovirus and purified as described previously (Redecke *et al.*, 2013) with the exception that the crystals were not crushed prior to measurements. These crystals have typical dimensions of 5–20 μm length and about 0.9 μm width, and they remain crystalline in a 1× phosphate buffered saline (PBS) suspension (137 mM NaCl, 2.7 mM KCl, 10 mM Na2HPO4, and 2 mM KH2PO4) after purification from the mother cells.

B. SFX experiment

The experiment was carried out using the nanofocus sample chamber of the coherent X-ray imaging instrument (Boutet and Williams, 2010) in June 2013 (Proposal No. L669). Two SFX datasets were collected from TbCatB crystals using 6 keV photons at two different X-ray fluences. A first dataset was collected with the incident X-ray beam attenuated, using silicon filters of different thicknesses, to between 1% and 27% of its full intensity. A second dataset was also collected using the full photon flux, and in this case the detector was protected by an attenuator placed one centimeter downstream of the interaction region to reduce the strong scattered signal that would have damaged the detector. The transmission of this attenuator was 25%, and specially designed to be constant over the 2ϑ scattering angle. The beamline efficiency was estimated to be around 20% at 6 keV, meaning that the average pulse energy at the sample was about 0.5 mJ. Assuming a circular focal spot size with 0.2 μm diameter, the pulse fluence for the unattenuated beam was nominally 1.1×10^{13} photons/μm^2.

A suspension of TbCatB crystals in 1× PBS buffer at pH 7.2, containing on the order of 10^9 crystals/ml, was passed through a 5 μm stainless steel inline filter. The crystal suspension was then delivered to the X-ray beam as a liquid jet of about 3–5 μm diameter produced with a gas dynamic virtual nozzle (DePonte *et al.*, 2008 and Weierstall *et al.*, 2012) and running with a flow rate between 10 and 25 μl/min. FEL pulses of nominal 60 fs duration were focused onto the liquid stream, about 50 μm away from the nozzle tip. Under these experimental conditions, about 3% of the recorded frames contained diffraction from TbCatB crystals (see Table I for data statistics).

TABLE I. SFX data statistics. The metrics were calculated considering Friedel pairs as distinct reflections.

	High fluence (HF)	*Low fluence (LF)*
Wavelength (Å)	2.066 (6 keV)	
Pulse fluence (photons/μm^2)	1.1×10^{13}	1.1×10^{11}–3.0×10^{12}
Dose (GGy/crystal)[a]	37	0.37–10
Space group	$P4_22_12$	
Unit cell dimensions (Å)	a = b = 124.4, c = 47.4	
Number of crystal hits	53 733	47 347
Number of indexed patterns (indexing rate)	37 389 (69.6%)	32 536 (68.7%)
Lowest/highest resolution (Å)	26.4/3.26	26.4/3.26
Completeness	100% (100%[b])	100% (100%[b])
I/σ(I)	5.19 (1.86[b])	5.86 (1.76[b])
R_{split} (%)[c]	18.1 (55.3[b])	14.8 (59.1[b])
CC[d]	0.96 (0.54[b])	0.97 (0.54[b])
Multiplicity	541 (513[b])	615 (566[b])

[a]Calculated by considering an average protein of density of 1.35 g cm^{-3}.
[b]Refers to the highest resolution shell (3.30 Å–3.22 Å).
[c]The definition of R_{split} is given in White *et al.* (2012).
[d]The Pearson correlation coefficient.

C. Data analysis

Figure 1 shows the effective scattering strength of sulfur atoms in the protein as a function of the peak fluence, as calculated using *XATOM* (Son *et al.*, 2011b). Here, the effective scattering strength is expressed in terms of the number of scattering electrons and defined as the root mean square of the time-dependent form factor during the XFEL pulse, weighted by the spatial and temporal X-ray beam profile (Galli *et al.* unpublished). The temporal profile was assumed to have a 60 fs flat-top shape. The scattering strength is highly dependent on the spatial X-ray beam profile in the interaction volume, and its upper limit was found in the case of spatially uniform fluence (solid line). The dashed line was calculated using a Gaussian spatial profile with a 0.2-μm FWHM. In this calculation, the sample was assumed to be considerably larger than the Gaussian spot, in which case the contribution of atoms in the sample to the effective scattering strength is weighted by the spatially varying fluence. The calculation equivalently represents the result of averaging diffraction intensities obtained from many smaller crystals that each randomly samples positions in the focused profile on different pulses. The dotted line of Figure 1 was obtained by assuming the same Gaussian profile and taking into account only the first 20 fs of the pulse, to simulate a possible self-gating effect of diffraction (Barty *et al.*, 2012 and Caleman *et al.*, 2015). From these calculations, it is expected that the resulting contrast in the effective scattering strength on the sulfur sites between HF (unattenuated beam) and the low-fluence (LF, attenuated beam) is in the range of +1.3 electrons to +8.0 electrons, depending on the interaction geometry and on possible self-gating effects.

A total of 101 080 images were identified as crystal hits by the program *Cheetah* (Barty *et al.*, 2014) and further processed by *indexamajig* from the CrystFEL suite (White *et al.*, 2013). Indexing trials were initially performed to optimize the unit cell parameters, starting from the values of a previously deposited structure (PDB code 4HWY) (Redecke *et al.*, 2013) and to refine the detector geometry. Randomly chosen diffraction patterns from each run were visually inspected to find possible regions of the detector to exclude from further analysis. The excluded regions contained, amongst other things, bright streaks close to the central beam caused by scatter from the water jet, shadows from the nozzle tip at high angles of diffraction, and features from the post-sample attenuator. In total, 37 389 and 32 536 diffraction patterns were successfully indexed for the HF and LF conditions, respectively. Monte Carlo integrated intensities were computed with *process_hkl* (White *et al.*, 2013), discarding reflections measured less than 11 times. Table I shows the detailed statistics of the two datasets collected as well as the values of some quality metrics determined from the final merged data. It can be seen from Figure 2 that because of the long wavelength and the experimental geometry, the diffracted intensity at high resolution is weak, and the I/σ(I) level (White *et al.*, 2013) decreases to below 2.0 at 3.26 Å, at which point R_{split} also starts to increase rapidly. The two data sets were therefore truncated at this limiting resolution.

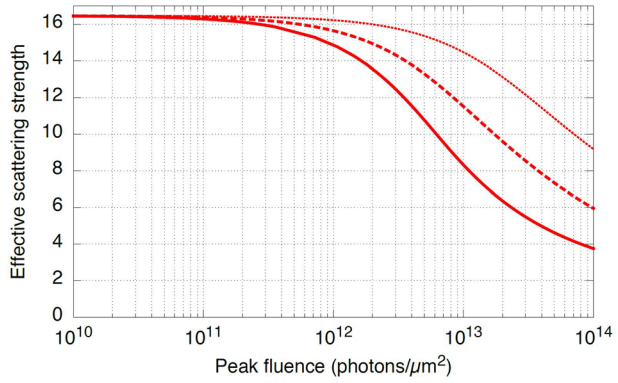

FIG. 1. The effective scattering strength of sulfur, calculated for a 60-fs flat-top pulse, as a function of the peak fluence. The solid line is calculated assuming a uniform spatial profile of the X-ray beam; the dashed line is the result of a Gaussian intensity profile; the dotted line is calculated with a Gaussian profile, only taking into account the first 20 fs pulse.

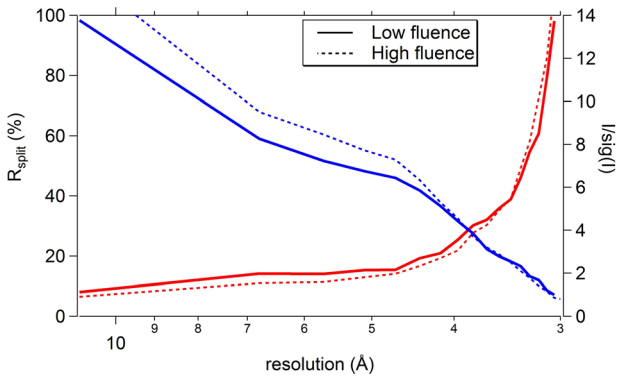

FIG. 2. The R_{split} and I/σ(I) metrics, in red and blue, respectively, from the low fluence (thick line) and high fluence (dashed line) datasets are shown as a function of resolution.

D. Substructure determination and phasing attempts

In order to measure relative differences due to the photoionization processes, the diffraction intensities of the two datasets were cross-scaled using *CCP*4 *Scaleit* (Howell and Smith, 1992). The low fluence data was treated as a "derivative" set, due to the expected higher scattering strength of the less-ionised atoms, while the high fluence data was treated as "native." The best scaling function was found using a final Wilson scaling performed after a least-squares determination of the isotropic temperature factors.

Initial evidence of a difference signal was obtained from a difference electron density map derived from difference structure factors *Fo*(*LF*)-*Fo*(*HF*) combined with the phases obtained from a molecular replacement run using the low fluence data, performed using *Phaser* (McCoy *et al.*, 2007). The search model was from PDB accession code 4HWY, and its refined version is superimposed on the map in Figure 3 to provide a visual reference. This figure shows that some of the strongest difference density (shown in green) corresponds to the sulfur positions, in particular, those belonging to the residues CYS 158, CYS 215, and MET 138. The highest of these peaks reaches a level of about 7σ.

A RIP approach was attempted, using the localized contrast on the sulfur positions, with no success. Similarly, conventional S-SAD phasing failed on both datasets, most probably due to the low resolution of the datasets and the insufficient data quality.

We then tried to quantify the electron density loss in the proximity of the sulfur atoms using occupancy refinement. Any excess photoionization of these atoms (compared to the

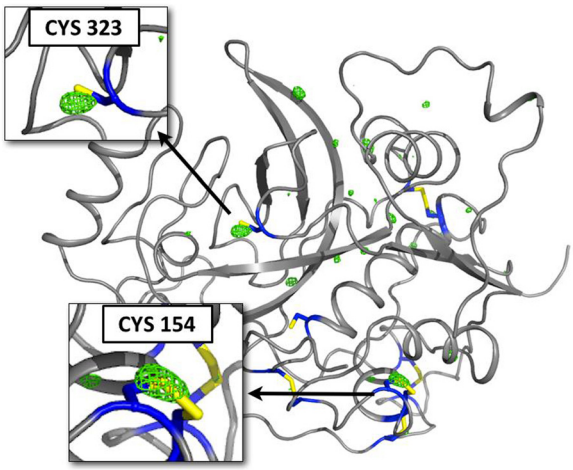

FIG. 3. Phased difference (Fo(LF)-Fo(HF)) Fourier map contoured at 4.5σ (green meshes) superposed to the TbCatB model, shown in grey. Sulfur atoms are represented by yellow sticks with a portion of the corresponding residue in blue.

average photoionization of all atoms) will result in a loss of scattering power of the sulfur species that will affect the diffraction pattern. A convenient way to quantify a relative change in the average electron density of each sulfur atom is to refine the occupancies of these atoms, keeping the B-factors of all atoms fixed. Although refinement of occupancy and B-factor is often degenerate, fixing one term allows a difference in electron density to be tracked. Ten parallel refinement runs on the experimental data were carried out using REFMAC5 (Murshudov *et al.*, 1997), where the initial occupancy of the S atoms of a previously refined model was varied from 0 to 1 in steps of 0.1. Figure 4 shows the average electron loss between low and high fluence, for each of the sulfur sites of the TbCatB (shown along the horizontal axis). The associated error bars indicate the standard deviation of the refinement results. Two sites, namely, MET 138 and MET 244, failed to produce meaningful results, either because the final occupancy was close to zero for most of the starting parameters (for MET 138) or because it failed to converge (MET 244), and are indicated with dotted lines. The graph shows an average positive difference of about 1.9 electrons, consistent with an increased ionization at high fluence and at the lower bound of the calculated contrast mentioned in Sec. II C. To test the efficacy of the occupancy refinement, the hardcoded form factor of sulfur in the CCP4 library was modified, adding two extra scattering electrons. The results are shown in the figure with pink circles.

The confidence of the results obtained was tested by performing a single sample t-test with a null-hypothesis, using the average occupancy change as input data. The test resulted in a statistical t value of 6.7, much higher that the critical value (2.1), which allowed the hypothesis that the results were obtained by chance to be excluded.

III. DISCUSSION AND CONCLUSION

The difference signals shown in Figures 3 and 4 give the first experimental evidence of a change in scattering strength of atoms in a protein crystal due to differences in the degree of ionization at different fluences of high-intensity X-ray FEL pulses. The largest changes are observed to be localised at the sulfur sites, due to the higher photoabsorption cross section of this atomic species with respect to the other atoms in the sample. However, the experiment was limited by the low number of indexed diffraction patterns and by the relatively low resolution of the datasets (3.26 Å), which prevented *de novo* phasing attempts from succeeding. Recent

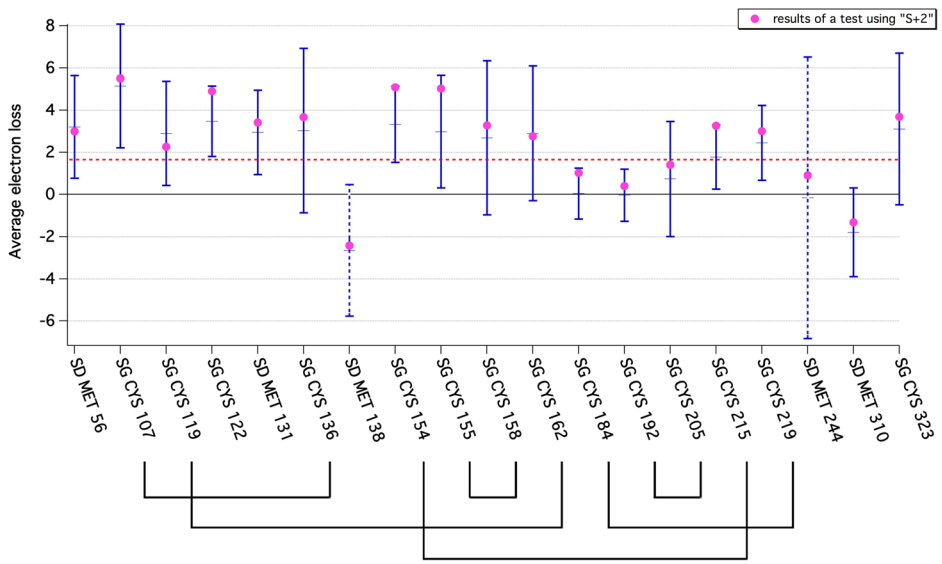

FIG. 4. The average electron loss around the sulfur sites, calculated from the difference in occupancy between the two datasets (low fluence and high fluence). The red dashed line represents the weighted average. The labels of the horizontal axis are consistent with those used in the deposited structure (4HWY.pdb). The dotted lines indicate that the refinement was found not to work for the corresponding sulfur sites. The black lines below the horizontal axis indicate S-S bridges present in the structure. The pink circles are the result of a test, where the form factor of sulfur was increased by 2 electrons.

simulations presented in the work of Galli *et al.* (2015) suggested, for the same model system, a minimum required RIP peak height of 16σ for experimental phasing to be successful. Under the conditions of the experiment reported here, we predict that about 200 000 diffraction patterns would be needed to achieve the required contrast. As already shown (Galli *et al.* submitted), by using particular criteria for selecting the best diffraction patterns, the difference of the average scattering strength of the heavy atoms between the LF and HF sets could be increased. This selection reduces the number of usable patterns, so it requires initial datasets containing a higher number of patterns: a condition that was not met in this experiment. Besides the criterion considered here of selecting the patterns according to the average integrated intensity of detected peaks as a function of the incoming pulse intensity, it might also be possible to choose patterns that show large differences of the intensity of selected Bragg reflections which are more sensitive to the scattering strength of the heavy atoms. This approach is, however, limited by the unknown degree of partiality of the reflections (Kirian *et al.*, 2010 and White *et al.*, 2013), an important factor affecting SFX data that can only be approximately modelled (Sauter, 2015). Further improvement in future experiments may come using extra diagnostics installed at the SFX experiment, to provide shot-by-shot information about the real fluence impinging on the crystal, such as a beam intensity monitor after the interaction region to measure the transmitted beam intensity or a simultaneous measurement of the fluorescence signal from the heavy atoms in the sample.

ACKNOWLEDGMENTS

Parts of this research were performed at the Linac Coherent Light Source, a National User Facility operated by Stanford University on behalf of the U.S. Department of Energy, Office of Basic Energy Sciences. The CXI instrument was funded by the LCLS Ultrafast Science Instruments (LUSI) project that was funded by the Office of Basic Energy Sciences of the U.S. Department of Energy. The Helmholtz Association through the Center for Free-Electron Laser Science and the PIER Helmholtz Graduate School, the Graduate College "GRK 1355" at the University of Hamburg, the Max-Plank-Society, the BMBF (projects 05K13GU7 and 05K13GU1) and the SIAS project (Grant No. 01KX0806/01KX0807), the Swedish research council and Swedish Foundation for Strategic Research, the German Academic Exchange Service (DAAD) through the RISE program, and the NSF STC Award No. 1231306 are acknowledged for financial support. We thank the staff at the LCLS for their excellent support. We acknowledge I. Schlichting, T. Barends, and R. Santra for fruitful discussions.

Barends, T. R., Foucar, L., Botha, S., Doak, R. B., Shoeman, R. L. *et al.*, "De novo protein crystal structure determination from X-ray free-electron laser data," Nature **505**(7482), 244–247 (2014).

Barty, A., Caleman, C., Aquila, A., Timneanu, N., Lomb, L., White, T. A. *et al.*, "Self-terminating diffraction gates femtosecond X-ray nanocrystallography measurements," Nat. Photonics **6**(1), 35–40 (2012).

Barty, A., Kirian, R. A., Maia, F. R. N. C., Hantke, M., Yoon, C. H., White, T. A., and Chapman, H. N., "Cheetah: Software for high-throughput reduction and analysis of serial femtosecond X-ray diffraction data," J. Appl. Crystallogr. **47**, 1118–1131 (2014).

Boutet, S. and Williams, G. J., "The coherent X-ray imaging (CXI) instrument at the Linac Coherent Light Source (LCLS)," New J. Phys. **12**, 035024 (2010).

Caleman, C., Timneanu, N., Martin, A. V., Jönsson, H. O., Aquila, A, Barty, A., Scott, H. A., White, T. A., and Chapman, H. N., "Ultrafast self-gating Bragg diffraction of exploding nanocrystals in an X-ray laser," Opt. Express **23**, 1213–1231 (2015).

DePonte, D. P., Weierstall, U., Schmidt, K., Warner, J., Starodub, D., Spence, J. C. H., and Doak, R. B., "Gas dynamic virtual nozzle for generation of microscopic droplet streams," J. Phys. D: Appl. Phys. **41**, 195505 (2008).

Galli, L., Son, S.-K., White, T. A., Santra, R., Chapman, H. N., and Nanao, M. H., "Towards RIP using free electron laser SFX data," J. Synchrotron Rad. **22**, 249–255 (2015).

Galli, L., Barends, T., White, T. A., Son, S.-K., Barty, A., Botha, S., Boutet, S., Doak, R. B., Nanao, M. H., Nass, K., Schoeman, R. L., Santra, R., Schlichting, I., and Chapman, H. N., "Towards phasing using high X-Ray intensity" (unpublished).

Howell, P. and Smith, G., "Identification of heavy-atom derivatives by normal probability methods," J. Appl. Crystallogr. **25**, 81–86 (1992).

Kirian, R. A., Wang, X., Weierstall, U., Schmidt, K. E., Spence, J. C., Hunter, M., and Holton, J., "Femtosecond protein nanocrystallography—Data analysis methods," J. Opt. Express **18**, 5713–5723 (2010).

McCoy, A. J., Grosse-Kunstleve, R. W., Adams, P. D., Winn, M. D., Storoni, L. C., and Read, R., "Phaser crystallographic software," J. Appl. Crystallogr. **40**, 658–674 (2007).

Murshudov, G. N., Vagin, A. A., and Dodson, E. J., "Refinement of macromolecular structures by the maximum-likelihood method," Acta Crystallogr., Sect. D: Biol. Crystallogr. **53**, 240–255 (1997).
Nass, K. *et al*., "Indications of radiation damage in ferredoxin microcrystals using high-intensity X-FEL beams," J. Synchrotron Rad. **22**, 225–238 (2015).
Ravelli, R. B. *et al*., "Specific radiation damage can be used to solve macromolecular crystal structures," Structure **11**, 217–24 (2003).
Redecke, L., Nass, K., DePonte, D. P., White, T. A., Rehders, D. *et al*.. "Natively inhibited Trypanosoma brucei Cathepsin B structure determined by using an X-ray laser," Science **339**, 227–230 (2013).
Sauter, N. K., "XFEL diffraction: developing processing methods to optimize data quality," J. Synchrotron Rad. **22**, 239–248 (2015).
Son, S.-K., Chapman, H. N., and Santra, R., "Multiwavelength anomalous diffraction at high x-ray intensity," Phys. Rev. Lett. **107**, 218102 (2011a).
Son, S.-K., Young, L., and Santra, R., "Impact of hollow-atom formation on coherent x-ray scattering at high intensity," Phys. Rev. A **83**, 033402 (2011b).
Weierstall, U., Spence, J. C. H., and Doak, R. B., "Injector for scattering measurements on fully solvated biospecies," Rev. Sci. Instrum. **83**, 035108 (2012).
White, T. A., Kirian, R. A., Martin, A. V., Aquila, A., Nass, K., Barty, A., and Chapman, H. N., "CrystFEL: A software suite for snapshot serial crystallography," J. Appl. Crystallogr. **45**, 335–341 (2012).
White, T. A., Barty, A., Stellato, F., Holton, J. M., Kirian, R. A., Zatsepin, N. A., and Chapman, H. N., "Crystallographic data processing for free-electron laser sources," Acta Crystallogr., Sect. D: Biol. Crystallogr. **69**, 1231 (2013).